BMC Plant Biology

RESEARCH

Open Access

Cellular messengers involved in the inhibition of the Arabidopsis primary root growth by bacterial quorum-sensing signal *N*-decanoyl-L-homoserine lactone

Xiang-yu Cao[1], Qian Zhao[1,2], Ya-na Sun[3], Ming-Xiang Yu[1], Fang Liu[1,2], Zhe Zhang[1], Zhen-hua Jia[1,2] and Shui-shan Song[1,2,4*]

Abstract

Background *N*-acyl-homoserine lactones (AHLs) are used as quorum-sensing signals by Gram-negative bacteria, but they can also affect plant growth and disease resistance. *N*-decanoyl-L-homoserine lactone (C10-HSL) is an AHL that has been shown to inhibit primary root growth in *Arabidopsis*, but the mechanisms underlying its effects on root architecture are unclear. Here, we investigated the signaling components involved in C10-HSL-mediated inhibition of primary root growth in *Arabidopsis*, and their interplay, using pharmacological, physiological, and genetic approaches.

Results Treatment with C10-HSL triggered a transient and immediate increase in the concentrations of cytosolic free Ca^{2+} and reactive oxygen species (ROS), increased the activity of mitogen-activated protein kinase 6 (MPK6), and induced nitric oxide (NO) production in *Arabidopsis* roots. Inhibitors of Ca^{2+} channels significantly alleviated the inhibitory effect of C10-HSL on primary root growth and reduced the amounts of ROS and NO generated in response to C10-HSL. Inhibition or scavenging of ROS and NO neutralized the inhibitory effect of C10-HSL on primary root growth. In terms of primary root growth, the respiratory burst oxidase homolog mutants and a NO synthase mutant were less sensitive to C10-HSL than wild type. Activation of MPKs, especially MPK6, was required for C10-HSL to inhibit primary root growth. The *mpk6* mutant showed reduced sensitivity of primary root growth to C10-HSL, suggesting that MPK6 plays a key role in the inhibition of primary root growth by C10-HSL.

Conclusion Our results indicate that MPK6 acts downstream of ROS and upstream of NO in the response to C10-HSL. Our data also suggest that Ca^{2+}, ROS, MPK6, and NO are all involved in the response to C10-HSL, and may participate in the cascade leading to C10-HSL-inhibited primary root growth in *Arabidopsis*.

*Correspondence:
Shui-shan Song
shuishans620@163.com
[1]Biology Institute, Hebei Academy of Sciences, 46th, South Street of Friendship, 050051 Shijiazhuang, Hebei, China
[2]Hebei Engineering and Technology Center of Microbiological Control on Main Crop Disease, 46th South Street of Friendship, Shijiazhuang, China
[3]College of Life Science, Hebei University, 180th East Road of Wusi, Baoding, China
[4]Hebei Collaboration Innovation Center for Cell Signaling Environmental Adaptation, 20 East NanErhuan Road, Shijiazhuang, China

Introduction

Many Gram-negative bacteria use *N*-acyl-homoserine lactones (AHLs) as signaling molecules for intercellular communication in a process known as quorum sensing (QS) [1–3]. To date, numerous AHL derivatives with acyl chains of different lengths (from 4 to 18 carbons) and substitutions of hydroxyl or oxo groups at the γ position of the carbon chain has been identified from more than 70 species of Gram-negative bacteria [2, 4]. AHL-mediated QS plays an essential role in many bacterial physiological processes including symbiosis, virulence, antibiotic production, extracellular polysaccharide production, resistance to oxidative stress, biofilm formation, and motility [5–7].

Plants can also sense and respond to bacterial QS signals [8–12]. For example, Mathesius et al. (2003) found that more than 150 proteins in *Medicago truncatula* changed in abundance after application of 3-oxo-*N*-(tetrahydro-2-oxo-3-furaryl)-hexadecenamide (3OC16-HSL) isolated from cultured *Sinorhizobium meliloti* [13]. Schuhegger et al. (2006) demonstrated that *N*-hexanoyl-homoserine lactone (C6-HSL) induces systemic accumulation of salicylic acid- and ethylene-dependent defense gene transcripts [14]. In *Arabidopsis,* *N*-3-oxo-tetradecanoyl-homoserine-lactone (3OC14-HSL) conferred resistance to biotrophic and hemibiotrophic pathogens *via* an oxylipin/SA-dependent pathway [9]. Whereas long-chain AHLs (side chains with 12–14 carbons) induce defense responses, short-chain AHLs (side chains with fewer than 8 carbons) promote elongation of the plant primary root. The G-protein-coupled receptor (GCR) and the transcription factor AtMYB44 were involved in the regulation of primary root growth by 3-oxo-octanoyl-homoserine lactone (3OC8-HSL) [15, 16].

Medium-chain AHLs, i.e., those with 10 carbon atoms in the carbon chain with or without substitutions at the γ position, have multiple functions in root morphogenesis, plant senescence, and defense responses [11, 17–20]. Hu et al. (2018) reported that *N*-decanoyl-homoserine lactone (C10-HSL) activates plant systemic resistance against *Botrytis cinerea* in tomato, and that C10-HSL-induced resistance is largely dependent on the jasmonic acid (JA) signaling pathway [19]. Ortiz-Castro et al. (2008) compared the effects of seven different AHLs on root architecture in *Arabidopsis* and found that C10-HSL had the strongest effect to inhibit primary root growth and promote lateral root formation [18]. Bai et al. (2012) found that an analog of C10-HSL, *N*-3-oxo-decanoyl-homoserine lactone (3OC10-HSL), mediated auxin-dependent adventitious root formation *via* H_2O_2- and nitric oxide (NO)-dependent cGMP signals in mung bean (*Vigna radiata*) seedlings [11]. However, the signaling pathway through which C10-HSL modulates plant primary root growth remains unclear.

Reactive oxygen species (ROS) and NO are important signals that participate in various physiological processes [14, 18, 21–26]. Zhang et al. (2017) found that ROS and NO were involved the inhibition of primary root growth by exogenous H_2S in *Arabidopsis* [27]. Treatments with C6-HSL, *N*-octanoyl-homoserine lactone (C8-HSL), C10-HSL, and *N*-decanoyl-homoserine-lactone (C12-HSL) led to NO accumulation in the calyptra and elongation zone of barley roots and altered root morphology [28]. Recently, we reported that pretreatment with 3OC8-HSL and subsequent pathogen invasion triggered an augmented ROS burst in *Arabidopsis* [29].

Mitogen-activated protein kinase (MAPK) cascades are highly conserved signal transduction pathways that participate in the regulation of growth and development and in responses to environmental stress in plants [30–34]. AtMPK3/6 regulate plant growth, development, and stress tolerance by interacting with Ca^{2+} and ROS pathways [31, 35–37]. Schikora et al. (2011) found that 3OC14-HSL pretreatment activated AtMPK3/6 upon challenge by flg22 in *Arabidopsis* [9].Calcium ions (Ca^{2+}) are a ubiquitous intracellular second messenger that participate in many signal transduction pathways in plants [38–41]. In our previous study, we found that C4-HSL induced a transient and immediate increase in the cytosolic free Ca^{2+} concentration ($[Ca^{2+}]_{cyt}$) in *Arabidopsis* [10]. Overall, data from the literature suggest that Ca^{2+}, ROS, NO, and MAPK participate in the plant's response to bacterial AHLs. However, the details of their involvement and the interplay among them in the regulation of primary root growth by C10-HSL is unknown. In this study, we investigated the involvement of intracellular Ca^{2+}, ROS, NO, and MPKs in C10-HSL-inhibited primary root growth in *Arabidopsis.* Our data indicate that C10-HSL inhibits primary root growth *via* a cascade involving Ca^{2+}, ROS, MAPK, and NO in *Arabidopsis.*

Results

C10-HSL influences *Arabidopsis* root system architecture

Previously, Ortiz-Castro et al. (2008) reported that C10-HSL is one of the most active AHLs tested to date, in terms of modification of *Arabidopsis* root system architecture [18]. In this study, we first confirmed the effects of C10-HSL on post-embryonic root development. We found that 10 nM to 1 μM C10-HSL treatment slightly caused a reduction in primary root growth and promoted lateral root formation (Fig. S1a, b). The primary root growth of plants treated with 15 to 75 μM C10-HSL was inhibited by 40–86% (Fig. 1a, b) and treatment 30 μM C10-HSL caused a 74% reduction in primary root length. Treatment with C10-HSL also resulted in significant increases in lateral root density and the density of

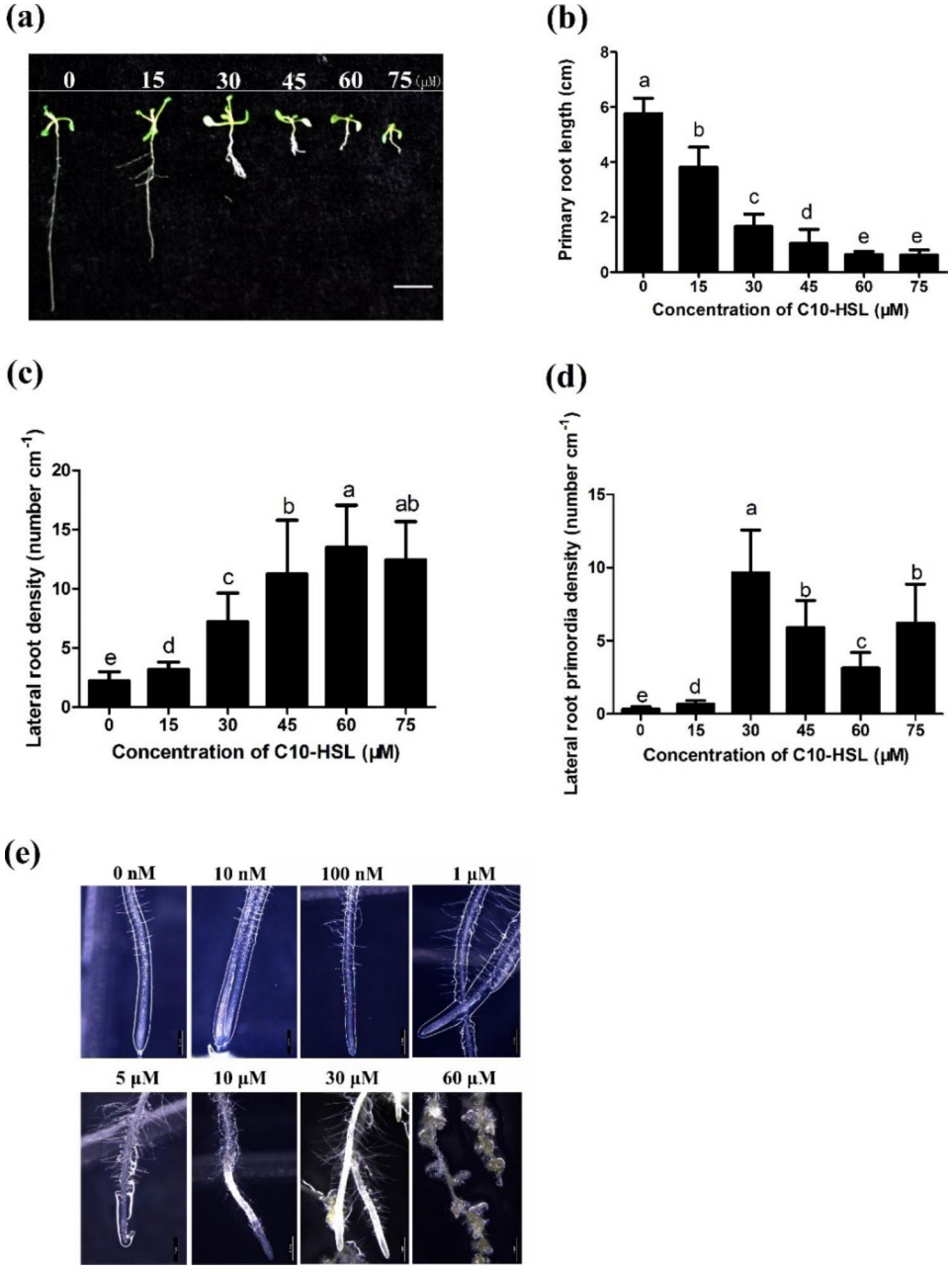

Fig. 1 *N*-decanoyl-homoserine lactone (C10-HSL) influences root system architecture in Arabidopsis. **(a)** Root architecture of wild-type (Col-0) Arabidopsis treated with different C10-HSL concentrations (0–75 μM), bar = 1 cm. **(b)** The effects of different C10-HSL concentration on primary root length, n = 40. **(c)** The effects of different C10-HSL concentration (0–75 μM) on lateral root density, n = 40. **(d)** The effects of different C10-HSL concentration (0–75 μM) on lateral root primordia density, n = 40. For the picture a-d, 3-d-old *Arabidopsis thaliana* seedlings were transferred to half-strength MS medium supplemented with the indicated concentrations of C10-HSL and grown for 5 d. **(e)** Representative photographs of root hairs formed at the primary root tip region of 3-day-old Arabidopsis seedlings grown in the presence of the indicated concentration of C10-HSL for 5 d, bar = 1 mm. All the error bars represent +/- SD. (Different letters indicate significantly different values, $P < 0.05$ by Tukey's test)

lateral root primordia (Fig. 1c–e and Fig. S1a). These data confirmed that C10-HSL can inhibit primary root growth and stimulate lateral root formation.

NO is involved in the inhibition of primary root growth by C10-HSL

Nitric oxide is an important gaseous signal that regulates root development [23, 42, 43]. To investigate the role of NO in C10-HSL-induced inhibition of primary root growth, we first measured NO production after C10-HSL treatment in *Arabidopsis* seedlings. Using

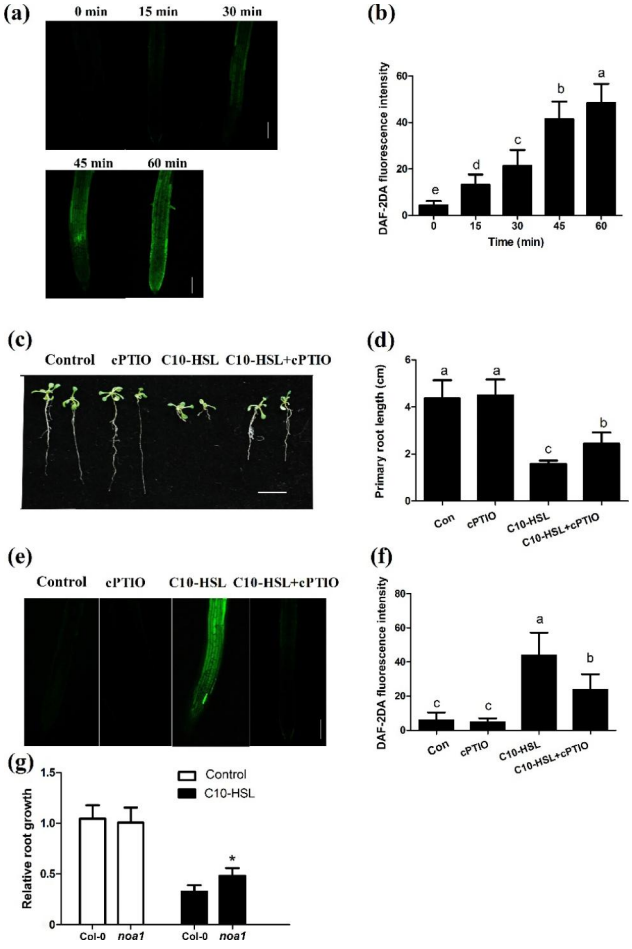

Fig. 2 NO is involved in the inhibition of primary root growth mediated by C10-HSL. **(a, b)** Detection of NO production in roots of Col-0 seedlings treated with C10-HSL (0–75 μM) for 0–60 min using the NO-specific fluorescent probe DAF-2DA (a) and quantification of NO-specific fluorescence intensities (b), bar = 50 μm, n = 30. **(c)**, Root architecture of wild-type Arabidopsis exposed to 30 μM C10-HSL with or without 100 μM cPTIO, bar = 1 cm. **(d)** Primary root length of wild-type seedlings exposed 30 μM C10-HSL with or without 100 μM cPTIO, n = 40. **(e, f)** Detection of NO production in roots of Col-0 seedlings treated as described in (c) using the NO-specific fluorescent probe DAF-2DA (e) and quantification of NO-specific fluorescence intensities (f). **(g)**, Relative primary root growth of wild-type and *noa1* exposed to 30 μM C10-HSL, n = 40. For the picture c, d and g, 3-d-old *Arabidopsis thaliana* seedlings were transferred to half-strength MS medium supplemented with the indicated concentrations of C10-HSL or other chemicals and grown for 5 d. Control or Con refers to solvent control. All the error bars represent +/- SD. (Different letters indicate significantly different values, $P < 0.05$ by Tukey's test; $^{*}P < 0.05$, $^{**}P < 0.001$, Student's t test)

the NO specific fluorescent probe diaminofluorescein diacetate (DAF-2DA), we found that C10-HSL elicited NO production in the roots within 15 min of treatment, and this effect lasted for 1 h or even longer (Fig. 2a, b). Supplementation with 100 μM 2-4-carboxyphenyl-4,4,5,5-tetramethylimidazoline-1-oxyl-3-oxide (cPTIO), an NO-specific scavenger, markedly alleviated the C10-HSL-induced inhibition of primary root growth (Fig. 2c, d). Consistent with the phenotypic results, NO production induced by C10-HSL treatment was significantly suppressed by cPTIO (Fig. 2e, f). We further analyzed the transcript levels of *NOA1*, encoding cGTPase [44], and *NIA1* and *NIA2*, encoding nitrate reductase, after treatment with C10-HSL in wild-type *Arabidopsis*. After C10-HSL treatment, the transcript level of *NOA1* increased within 1 h, peaked at 6 h after treatment, and then gradually declined (Fig. S2f). Similarly, the transcript levels of *NIA1* and *NIA2* increased within 1 h of treatment with C10-HSL in *Arabidopsis* roots (Fig. S2a, b). Seedlings of the *noa1* mutant were less sensitive to C10-HSL treatment with respect to primary root growth (Fig. 2 g). Likewise, *nia1* and *nia2* single mutants and *nia1nia2* double mutants were less sensitive to inhibition of primary root growth by C10-HSL (Fig. S3e). Collectively, these data suggest that NO is involved in the C10-HSL-mediated inhibition of primary root growth.

ROS are essential in C10-HSL-induced inhibition of primary root growth

In plants, ROS play an essential role in root growth and development [25, 45, 46]. To investigate the role of ROS in C10-HSL-mediated inhibition of primary root growth, we determined their levels in C10-HSL-treated seedlings using the ROS-specific fluorescent probe 2',7'-dichlorofluorescein diacetate (DCF-DA). The ROS levels in wild-type seedlings treated with 30 μM C10-HSL increased and peaked at 15 min after treatment (Fig. 3a, b). One important component of ROS is H_2O_2, which can be scavenged by catalase (CAT). When CAT was added to the medium containing 30 μM C10-HSL, the ROS level was 30% lower than that in the control (solvent-treated) seedlings (Fig. 3c, d). Then, we examined primary root elongation in wild-type seedlings treated with 30 μM C10-HSL in the presence or absence of exogenous H_2O_2 and CAT. We found that the C10-HSL-induced inhibition of primary root growth was increased by exogenous H_2O_2, but alleviated by CAT (Fig. 3e, f). The effect of C10-HSL on primary root growth was similar to that of H_2O_2, because addition of H_2O_2 alone significantly inhibited primary root growth (Fig. 3e, f). To verify the role of ROS in C10-HSL-mediated primary root growth inhibition, we analyzed the *Arabidopsis* ROS-biosynthesis-related respiratory burst oxidase homolog (Rboh) NADPH oxidase double mutant *rbohD/F*. In terms of the inhibition of primary root growth, *rbohD/F* plants were less sensitive to C10-HSL treatment than were wild-type plants (Fig. 3 g). These data indicate that ROS plays an essential role in the modulation of root growth by C10-HSL.

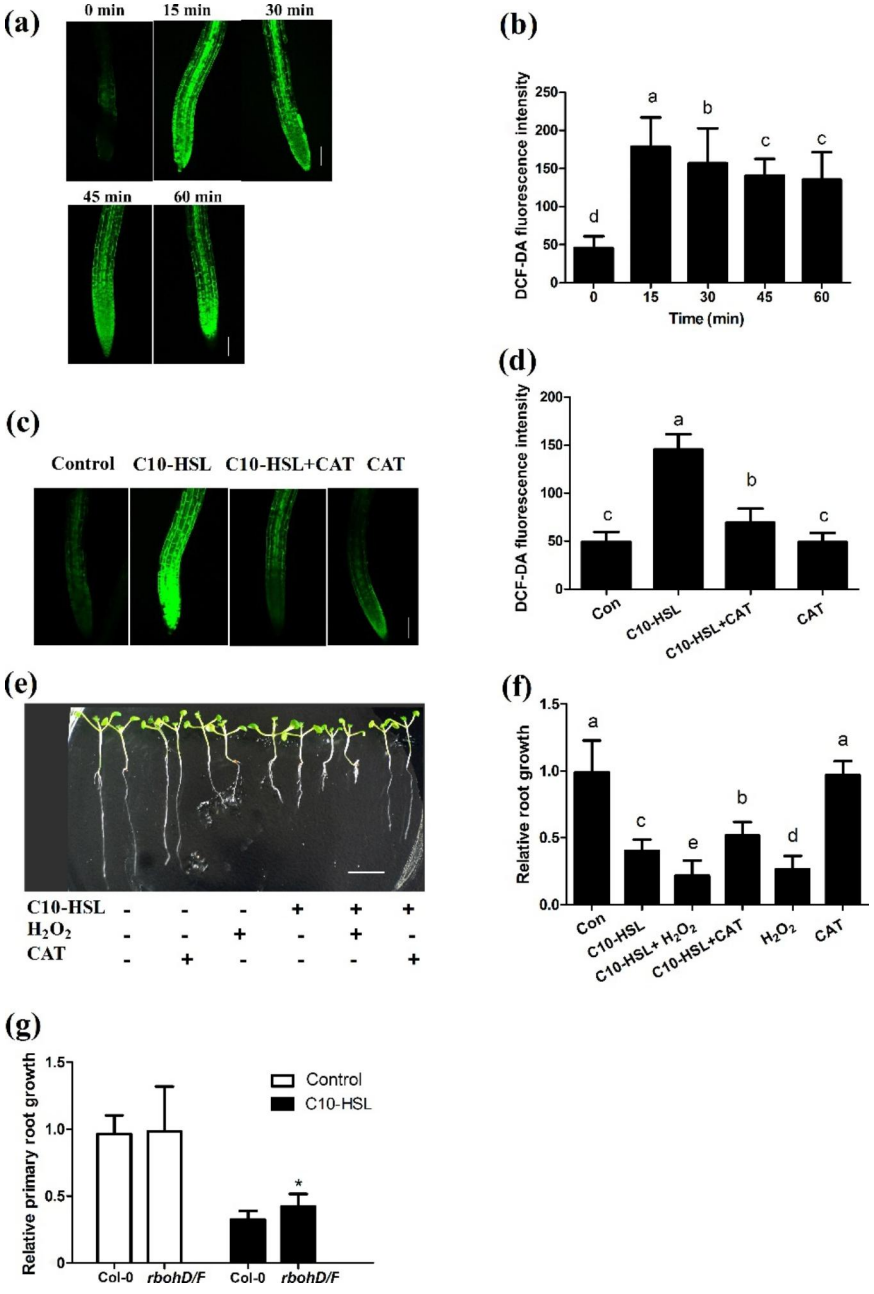

Fig. 3 ROS is involved in C10-HSL-mediated inhibition of primary root growth. **(a, b)** Detection of ROS level in the roots of wild-type seedlings exposed to 30 μM C10-HSL for 0–60 min using the ROS-specific florescent probe DCF-DA (a), and quantification of ROS-specific fluorescence intensities (b) bar = 50 μm. **(c, d)** Detection of ROS level in the roots of wild-type seedlings exposed to 30 μM C10-HSL with or without 500 μM CAT for 15 min using the ROS-specific florescent probe DCF-DA (c), and quantification of ROS-specific fluorescence intensities (d), n = 30, bar = 50 μm. **(e, f)** Relative primary root growth of wild-type seedlings exposed to 30 μM C10-HSL with or without 1.5 mM H_2O_2 and 500 μM CAT for 5 d, bar = 1 cm, n = 40. **(g)** Relative primary root growth of Col-0 and *noa1* seedlings exposed to 30 μM C10-HSL for 5 d, n = 40. Control or Con refers to solvent control. All the error bars represent +/- SD. (Different letters indicate significantly different values, $P < 0.05$ by Tukey's test. *$P < 0.05$, **$P < 0.001$, Student's t test)

MAPKs participate in the inhibition of primary root growth by C10-HSL

Previous studies have shown that MPK3/6 participate in the induction of the defense response by 3OC14-HSL in *Arabidopsis* [9], and that MPK4 regulates primary and lateral root growth [47, 48]. To investigate whether MAPKs play roles in the C10-HSL-induced inhibition of primary root growth, we first assessed the effects of U0126, a selective inhibitor of MAPK, on primary root elongation in wild-type *Arabidopsis* (Columbia-0). Addition of U0126 alleviated the C10-HSL-induced inhibition of primary root growth (Fig. 4a, b) and this effect

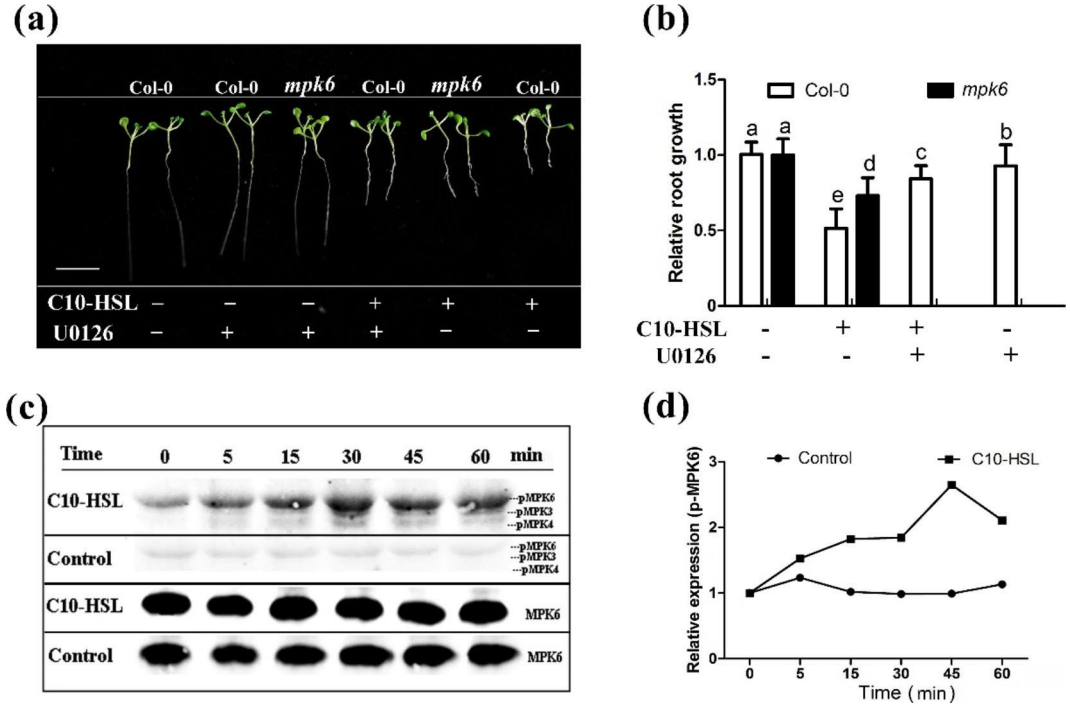

Fig. 4 MAPKs participates in the inhibition of primary root growth by C10-HSL. **(a, b)** Relative primary root growth of Col-0 and *mpk6* seedlings exposed to 30 μM C10-HSL with(+) or without(-) 20 μM U0126 (MAPK inhibitor) for 5 d, n = 40, bar = 1 cm. **(c)** Phosphorylation status (pMPK6, pMPK3 and pMPK4) and total MPK6 expression level in wild-type seedlings exposed to 30 μM C10-HSL or Control for 0–60 min. **(d)** Relative expression of pMPK6 in wild type seedlings treated with or without 30 μM C10-HSL for 0–60 min. Control or Con refers to solvent control. All the error bars represent +/- SD (Different letters indicate significantly different values, $P < 0.05$ by Tukey's test)

was dose-dependent (Fig. S3a, b). Western blotting using an anti-phosphate antibody showed that, compared with wild-type seedlings in the control, wild-type seedlings treated with C10-HSL had stronger phosphorylation activity of MPK6, which started at about 5 min and peaked at 45 min after C10-HSL treatment (Fig. 4c, d and Fig. S5 a-d). We also found that MPK3 and MPK4 in *Arabidopsis* were weakly activated from 30 to 60 min after treatment with 30 μM C10-HSL (Fig. 4c, d).

To confirm the involvement of MAPK in the response to C10-HSL, the effects of C10-HSL on primary root growth were compared between wild-type and *mpk6 Arabidopsis* seedlings. The inhibitory effect of C10-HSL on primary root growth was significantly alleviated in the *mpk6* mutant compared with the wild-type seedlings (Fig. 4a, b). Taken together, these results indicate that MAPKs, especially MPK6, are involved in the inhibition of primary root growth modulated by C10-HSL.

MPK6 mediates the C10-HSL-induced inhibition of primary root growth downstream of ROS and upstream of NO

On the basis of the data presented above, we concluded that ROS, NO, and MPK6 are important intermediate components in the regulation of primary root growth by C10-HSL. To explore the interplay among these components, we first detected the effect of the ROS scavenger CAT on the activation of MPK6 induced by C10-HSL. We found that the addition of CAT significantly decreased the activation of MPK6 by C10-HSL (Fig. 5a and Fig. S6 a-c). Next, we measured ROS and NO production in the mutants *noa1* and *rbohD/F*, respectively, after C10-HSL treatment. We found that C10-HSL-induced NO production was abolished in the *rbohD/F* mutant, while C10-HSL-induced ROS production was similar between wild-type and *noa1* (Fig. 5b, c). In addition, the ROS production induced by C10-HSL treatment was unaffected in the *nia1* and *nia2* single mutants and in the *nia1/2* double mutant (Fig. S2d). Further, qRT-PCR analyses showed that the induction of *noa1* expression by C10-HSL in wild-type plants was suppressed in mutant *rbohD/F* seedlings after exposure to C10-HSL (Fig. 5d). These data suggest that C10-HSL induces ROS production upstream of MAPK6 activation and NO accumulation in *Arabidopsis* roots.

We further checked the NO and ROS production in roots of *Arabidopsis mpk6* mutant seedlings. The induction of NO production by C10-HSL in wild-type seedlings was completely abolished in *mpk6* seedlings (Fig. 5f). In contrast, ROS accumulation in response to C10-HSL treatment was comparable between *mpk6* and wild-type plants (Fig. 5 g). Supplementation with CAT alleviated the C10-HSL-induced inhibition of primary

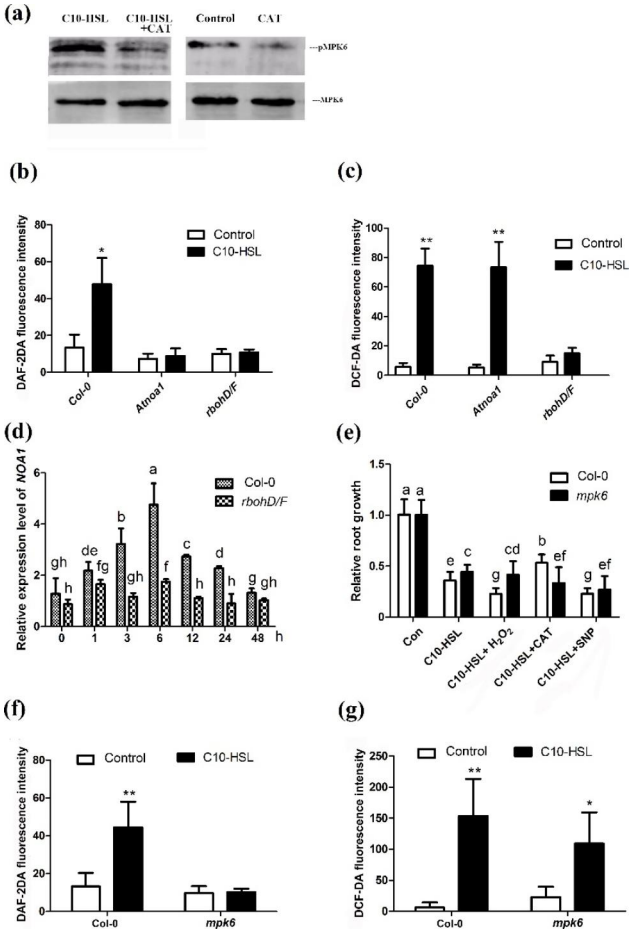

Fig. 5 MPK6 mediates the C10-HSL-induced inhibition of primary root growth downstream of ROS and upstream of NO. **(a)** Phosphorylation status (pMPK6) and total expression level of MPK6 in wild-type seedlings exposed to 30 μM C10-HSL with or without 500 μM CAT for 45 min. **(b)** Quantification of NO-specific fluorescence intensities in the roots of Col-0, *rbohD/F* and *noa1* seedlings exposed to 30 μM C10-HSL 1 h using the NO specific florescent probe DAF-2DA. **(c)** Quantification of ROS-specific fluorescence intensities in the roots of Col-0, *rbohD/F* and *noa1* seedlings exposed to 30 μM C10-HSL 15 min using the ROS specific florescent probe DCF-DA. **(d)** Transcriptional regulation of *NOA1* gene after exposed to 30 μM C10-HSL for up to 2 day in Col-0 and *rbohD/F*. **(e)** Relative root growth of Col-0 and *mpk6* seedlings exposed to 30 μM C10-HSL with or without 30 μM SNP, 1.5 mM H_2O_2 and 500 μM CAT for 5 d compared with untreated seedlings, n = 40. **(f)** Quantification of NO-specific fluorescence intensities in the roots of Col-0 and *mpk6* seedlings exposed to 30 μM C10-HSL 1 h using the NO specific florescent probe DAF-2DA. (**g**) Quantification of ROS-specific fluorescence intensities in the roots of Col-0 and *mpk6* seedlings exposed to 30 μM C10-HSL 15 min using the ROS specific florescent probe DCF-DA. Control or Con refers to solvent control. All the error bars represent +/- SD. (Different letters indicate significantly different values, $P < 0.05$ by Tukey's test)

root growth in wild-type roots, but did not further alleviate the C10-HSL-induced inhibition of primary root growth in the *mpk6* mutant (Fig. 5e). In contrast, supplementation with exogenous H_2O_2 exacerbated the C10-HSL-mediated inhibition of primary root growth in wild-type seedlings, but did not further increase the inhibitory effects of C10-HSL on primary root growth in the *mpk6* mutant (Fig. 5e). Supplementation with the NO donor sodium nitroprusside (SNP) increased the inhibitory effects of C10-HSL on the primary root growth of both *mpk6* and wild-type seedlings (Fig. 5e). Considering all these results, we concluded that MPK6 mediates the C10-HSL-induced inhibition of primary root growth downstream of ROS and upstream of NO.

C10-HSL triggers an elevated concentration of intracellular calcium and controls ROS and NO accumulation

Cytosolic Ca^{2+} is a second messenger that plays an essential role in plant root growth [49, 50]. The effect of C10-HSL on $[Ca^{2+}]_{cyt}$ was evaluated in root cells of transgenic *Arabidopsis* expressing the gene encoding intracellular apoaequorin. The results showed that the $[Ca^{2+}]_{cyt}$ level in *Arabidopsis* root cells significantly increased within 30 s of adding C10-HSL at concentrations from 10 nM to 30 μM (Fig. 6a). Pretreatments with La^{3+}, verapamil, or EGTA blocked the elevation in $[Ca^{2+}]_{cyt}$ caused by 30 μM C10-HSL (Fig. 6b). To further monitor whether C10-HSL affects the level of $[Ca^{2+}]_{cyt}$ in root cells, the fluorescence of the Ca^{2+}-sensitive dye Fluo-4 AM was analyzed by confocal microscopy. The fluorescence intensity level significantly increased after exposure to C10-HSL at concentrations higher than 100 nM in a dose-dependent manner (Fig. 6c, d). These data suggested that C10-HSL immediately triggers an elevation of $[Ca^{2+}]_{cyt}$ in *Arabidopsis* root cells. LiCl, a known inhibitor of the phosphatidylinositol cycle, inhibits the release of Ca^{2+} from intracellular calcium pools, while $LaCl_3$ inhibits the import of Ca^{2+} across the plasma membrane. Addition of both these compounds to the medium containing C10-HSL buffered its inhibitory effect on primary root growth in wild-type seedlings (Fig. 7a and Fig S4), implying that Ca^{2+} plays a role in C10-HSL-induced inhibition of primary root growth in *Arabidopsis.* To investigate whether Ca^{2+} affects ROS and NO production induced by C10-HSL, we measured the fluorescence intensity of DCF-DA as well as DAF-2DA and found that the addition of Ca^{2+} inhibitors down-regulated both ROS and NO production induced by C10-HSL, consistent with the decrease in $[Ca^{2+}]_{cyt}$ detected by Fluo-4 AM analyses (Fig. 7b–d). Taken together, these results indicate that C10-HSL increases the intracellular calcium concentration and controls the production of both ROS and NO.

Discussion

Many Gram-negative bacteria can use AHLs as intracellular signals to monitor their population density by QS [1–3]. AHLs not only play an essential role in QS-mediated physiological processes, but also modulate plant growth, defense responses, and development [11, 17, 18, 51–53]. C10-HSL or 3OC10-HSL can be produced

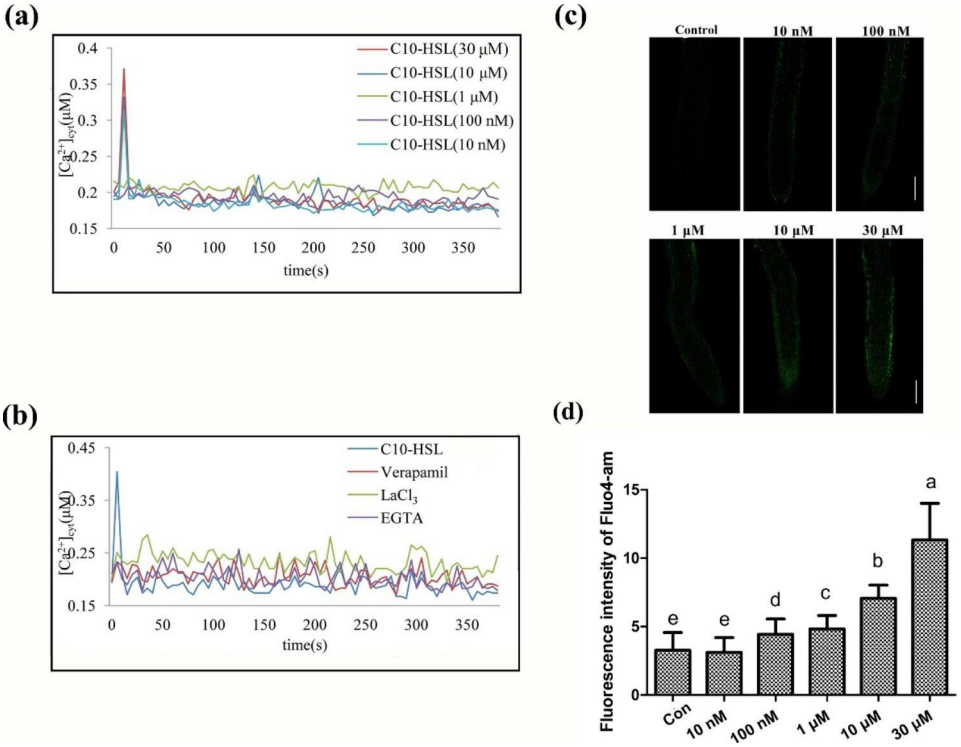

Fig. 6 C10-HSL improved cytosolic Ca^{2+} concentration in wild-type seedlings. **(a)** Changes in $[Ca^{2+}]_{cyt}$ in apoaequorin-transformed Arabidopsis root cells with 10 nM, 100 nM, 1 μM, 10 μM, 30 μM C10-HSL. **(b)** Changes in $[Ca^{2+}]_{cyt}$ in Arabidopsis root cells were measured upon addition of 30 μM C10-HSL after pretreatment with $LaCl_3$, EGTA and Verapamil respectively. **(c, d)** Detection of cytosolic Ca^{2+} concentration in the roots of Col-0 seedlings exposed to 0 nM, 10 nM, 100 nM, 1μM, 10 μM and 30 μM C10-HSL using the Ca^{2+} specific florescent probe Fluo4-am, bar = 100 μm. Control or Con refers to solvent control. All the error bars represent +/- SD. (Different letters indicate significantly different values, $P < 0.05$ by Tukey's test)

by several bacteria including the rhizosphere-colonizing bacteria *Pseudomonas fluorescens* and *Pseudomonas putida* [54], the nitrogen-fixing bacterial symbiont *Sinerhizobium meliloti* [55], and the pathogenic bacteria *Burkholderia pseudomallei* and *Burkholderia mallei* [2]. The concentration of AHLs in natural niches is estimated to range from 1 nM to 10 μM in the bulk rhizosphere, although the concentrations can be higher (>50 μM) in bacterial biofilms [56, 57]. Ortíz-Castro et al. (2008) tested the effects of seven AHLs with concentrations ranging from 12 to 192 μM on root growth, and found that C10-HSL showed the strongest effect to inhibit primary root growth and stimulate lateral root formation and root hair development [18]. A derivative of C10-HSL, 3OC10-HSL, was found to stimulate adventitious root formation in mung bean [11]. In this study, we confirmed the effect of C10-HSL and showed that treatment with 10 nM to 1 μM C10-HSL significantly reduced primary root growth and promoted lateral root formation. The effect of C10-HSL on root system architecture was concentration-dependent, and 30 μM C10-HSL caused a 74% reduction in primary root length that was accompanied by 3.5-fold increase in lateral root formation. These results were consistent with those reported by Bai et al. (2012) [11] and Ortíz-Castro et al. (2008) [18], and confirm that AHLs can mediate cross-kingdom interactions by modulating root development during the plant-bacteria interaction. Here, we focused on primary root growth and chose 30 μM C10-HSL as the effective concentration for further analyses. This concentration is somewhat higher than that produced by bacteria in the bulk rhizosphere but comparable to that present in bacterial biofilms.

In plants, ROS are involved in the responses to various phytohormones and environmental cues. We found that treatment with 30 μM C10-HSL increased ROS accumulation in roots, and this led to inhibition of primary root growth in *Arabidopsis*. The inhibitory effect of C10-HSL on primary root growth was alleviated by supplementation with CAT, but exaggerated by exogenous H_2O_2. This indicated that H_2O_2, one component of ROS, contributes to C10-HSL-mediated primary root growth inhibition in *Arabidopsis*. Further evidence was obtained from genetic analyses of the ROS-related mutant *rbohD/F*. We found that the primary roots of *rbohD/F* seedlings were less sensitive to C10-HSL treatment. Zhang et al. (2017) reported that ROS generation is required for exogenous H_2S-induced inhibition of primary root growth in *Arabidopsis* [27]. Similarly, ROS were found to accumulate in the root tips after treatment with the nitrification inhibitor methyl 3-(4-hydroxyphenyl) propionate (MHPP),

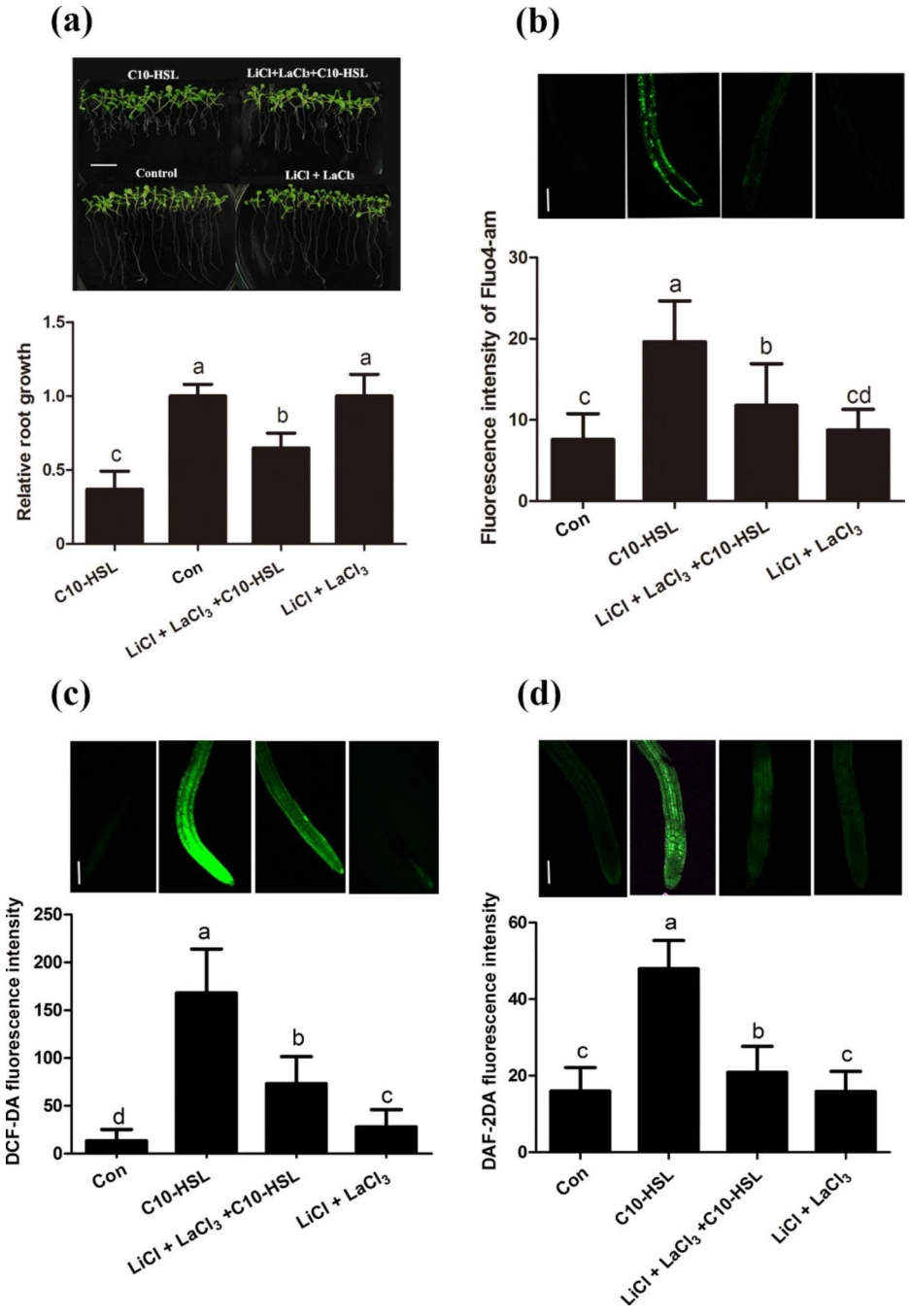

Fig. 7 Up-regulated cytosolic Ca^{2+} induced ROS and NO reaction which is necessary for C10-HSL induced root growth inhibition. **(a)** Relative primary root growth of Col-0 seedlings exposed to 30 μM C10-HSL with or without 100 μM LiCl plus 300 μM $LaCl_3$ compared with control for 5 d, bar = 1 cm, n = 40. **(b)** Detection of cytosolic Ca^{2+} concentration in the roots of Col-0 seedlings exposed to 30 μM C10-HSL with or without 100 μM LiCl plus $LaCl_3$ compared with untreated seedlings using the Ca^{2+} specific florescent probe Fluo4-am and quantification of Ca^{2+}-specific fluorescence intensities, bar = 100 μm, n = 30. **(c)** Detection of ROS production in the roots of Col-0 seedlings exposed to 30 μM C10-HSL with or without 100 μM LiCl plus $LaCl_3$ for 15 min using the specific florescent probe DCF-DA and quantification of specific fluorescence intensities, bar = 100 μm, n = 30. **(d)** Detection of NO production in the roots of Col-0 seedlings exposed to 30 μM C10-HSL with or without 100 μM LiCl plus $LaCl_3$ for 15 min using the NO specific florescent probe DAF-2DA and quantification of NO-specific fluorescence intensities, bar = 100 μm, n = 30. Control or Con refers to solvent control. All the error bars represent +/- SD. (Different letters indicate significantly different values, $P < 0.05$ by Tukey's test)

which inhibited primary root elongation in *Arabidopsis* [58]. These data show that AHLs influence primary root growth by regulating ROS accumulation in plant roots.

Another important signaling molecule is NO, which regulates root growth in plants. As AHL homologs, plant alkamides were found to induce accumulation of NO and

promote adventitious root development in *Arabidopsis thaliana* explants [59]. Pharmacological analyses indicated that blocking the 3OC8-HSL-induced accumulation of NO with the NO scavenger cPTIO significantly reduced the effect of 3OC10-HSL to stimulate adventitious root formation in mung bean, suggesting a role of NO in 3OC10-HSL-mediated root development [11]. In our experiments, we found that C10-HSL triggered NO accumulation in root tips. Moreover, supplementation with an NO scavenger abolished the production of NO induced by C10-HSL, and repressed the inhibitory effects of C10-HSL on primary root growth. Furthermore, we found that *NOA1 and NIA* were upregulated by C10-HSL, and that C10-HSL-mediated primary root growth inhibition was markedly impaired in the *NOA1*-defective mutant *noa1 and NIA* mutant *nia1nia2*. These results provide pharmacological and genetic evidence that NO is required for C10-HSL-inhibited primary root growth in *Arabidopsis*. Heavy metals such as zinc and cadmium and toxic chemicals including H_2S and MHPP inhibit primary root growth by increasing the concentration of intracellular NO, suggesting that NO is also involved in inhibiting primary root growth in response to environmental factors [27, 58].

In plants, MAPKs are activated in response to a number of environmental cues [60–62]. In this study, the MAPK inhibitor U0126 neutralized the C10-HSL-induced inhibition of primary root growth, and C10-HSL treatment strongly activated MPK6 and weakly activated MPK3 and MPK4 within 30 min. These findings indicate that activation of MAPK is required for the inhibition of primary root growth by C10-HSL. Consistent with this result, an MPK6 mutant showed reduced inhibition of primary root growth after C10-HSL treatment, providing molecular evidence for the essential role of MPK6 in C10-HSL-mediated inhibition of primary root growth. Previously, Schikora et al. (2011) reported that application of 3OC14-HSL induces resistance against bacterial and fungal pathogens, and this effect depends on strong and prolonged activation of MPK6 in *Arabidopsis* [9]. Accordingly, these data show that MPK6 is required for AHL-mediated changes in primary root growth.

MPK6 modulates plant growth and the response to environmental stimuli by interacting with ROS and/or NO [36, 37, 63, 64]. In *Arabidopsis*, NO stimulates cadmium-induced programmed cell death by enhancing MPK6-mediated caspase-3-like activation [65]. Compared with wild-type, the MPK6 mutant formed more and longer lateral roots after application of SNP but H_2O_2, indicating that MPK6 modulates NO accumulation and responses to H_2O_2 during root development in *Arabidopsis* [63]. Liu et al. (2016) reported that NO/ROS accumulation contributes to MHPP-mediated primary root growth inhibition and NO acts upstream of ROS in the response to MHPP in *Arabidopsis* [58]. Using pharmacological approaches, Bai et al. (2012) showed that H_2O_2 may modulate the NO signal during the response to 3OC10-HSL treatment in mung bean [11]. The results of those studies suggest that MPK6, ROS, and NO interact, but the mechanism underlying this interaction may be context-dependent. In this study, we observed that reducing ROS accumulation with the H_2O_2 scavenger CAT significantly decreased the activation of MPK6. We also found that C10-HSL-induced NO production was abolished in the *rbohD/F* mutant, while C10-HSL-induced accumulation of ROS was unaffected in the *noa1* mutant. In addition, C10-HSL treatment did not upregulate *NOA1* in the *rbohD/F* mutant. The induction of NO production by C10-HSL was completely abolished in the *mpk6* mutant, while ROS accumulation caused by C10-HSL treatment was unaffected. Addition of CAT did not further alleviate the C10-HSL-induced inhibition of primary root growth in roots of the *mpk6* mutant. In contrast, the defect in the C10-HSL-induced inhibition of primary root growth in the *mpk6* mutant was rescued by application of SNP, an NO donor, but not by addition of exogenous H_2O_2. Our data indicate that ROS, MPK6, and NO might work together to regulate plant root responses to C10-HSL. A similar signaling pathway has been reported to participate in the plant response to H_2S toxicity [27].

In plants, Ca^{2+} functions as an intracellular second messenger, and is essential for signal transduction processes [40, 41]. In our previous study, we showed that C4-HSL triggered an increase in the concentration of intracellular Ca^{2+} [9]. In the present study, we found that treatment with C10-HSL resulted in a transient and immediate increase in $[Ca^{2+}]_{cyt}$ in root cells of *Arabidopsis*. The effect of C10-HSL to increase the $[Ca^{2+}]_{cyt}$ concentration was investigated using the Ca^{2+}-sensitive dye Fluo-4 AM. These analyses showed that the inhibition of the increase in the intracellular Ca^{2+} concentration reduced the inhibitory effect of C10-HSL on primary root growth. Moreover, the addition of a Ca^{2+} inhibitor significantly reduced the production of ROS and NO induced by C10-HSL. Our data indicate that Ca^{2+} signaling may be an early event in the plant response to C10-HSL, and it may regulate the down-stream production of ROS. These mechanisms also occur during incompatible host-pathogen recognition, when the flux of Ca^{2+} across the plasma membrane is one of the earliest cellular events and results in a set of oxidative bursts that produce ROS [66, 67].

In conclusion, our results show that C10-HSL triggered a transient and immediate increase in the concentration of cytosolic free Ca^{2+} and induced ROS accumulation, MPK6 activation, and NO production in *Arabidopsis* primary roots. The generation of ROS and NO induced by

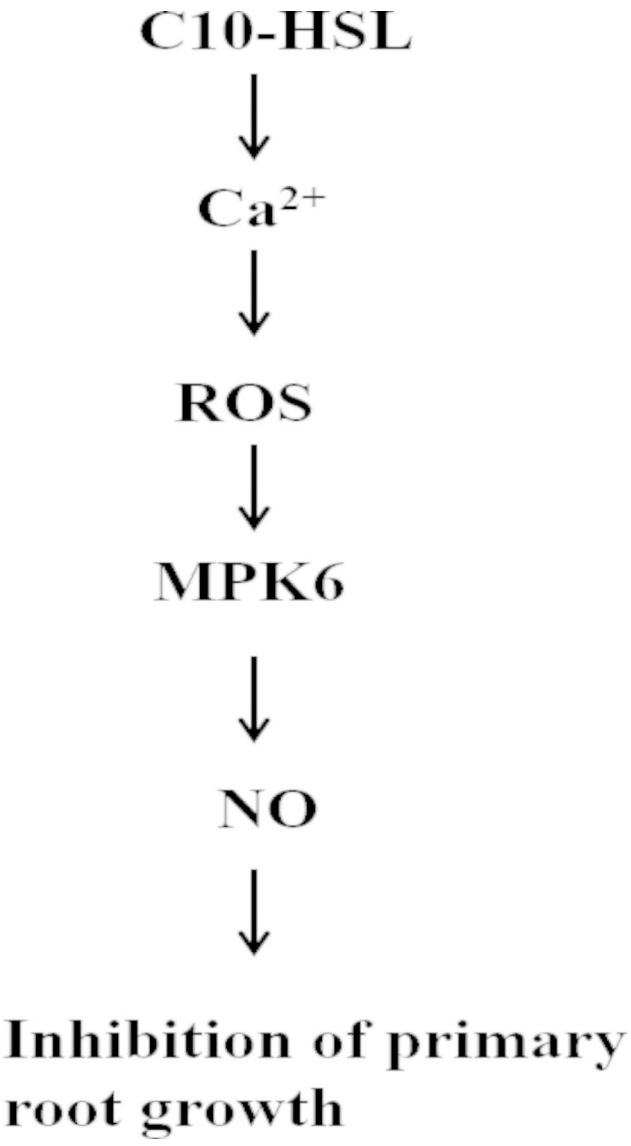

Fig. 8 The tentative model for C10-HSL-induced inhibition of primary root growth. C10-HSL triggered cytosolic free Ca^{2+} and reactive oxygen species (ROS), increased the activity of mitogen-activated protein kinase 6 (MPK6), and induced nitric oxide (NO) production in *Arabidopsis*, and finally inhibited primary root growth

C10-HSL was mediated by Ca^{2+}. Activation of MPKs was necessary for the inhibition of primary root growth by C10-HSL. MPK6 was shown to act downstream of ROS and upstream of NO. Thus, our data suggest that Ca^{2+}, ROS, MPK6, and NO are all involved and might play roles in cascade in the C10-HSL-mediated inhibition of primary root growth in *Arabidopsis* (Fig. 8). Auxin plays a fundamental role in root system architecture in plants [68, 69]. However, Ortiz-Castro et al. (2008) pointed out that C10-HSL is independent of auxin signaling in *Arabidopsis*, although the C10-HSL-mediated inhibition of primary root growth is similar to the typical auxin signaling phenotype [18]. However, 3OC12-HSL and 3OC16-HSL were found to induce the tissue-specific expression of auxin-responsive *GH3* in legume [13]. Bai et al. (2012) reported that 3OC10-HSL, an analog of C10-HSL, was able to mediate auxin-dependent adventitious root formation *via* H_2O_2- and NO-dependent cGMP signaling in mung bean seedlings [11]. C6-HSL was found to promote root elongation and increase the ratio of auxin: cytokinin towards higher auxin levels in both leaves and roots of *Arabidopsis* [51]. Zhang et al. (2017) reported that exogenous H_2S repressed the distribution of auxin and inhibited primary root growth in *Arabidopsis* [27]. The nitrification inhibitor MHPP was found to modulate root system architecture *via* ROS/NO-mediated-accumulation and redistribution of auxin in *Arabidopsis* roots [60]. Moreover, Hu et al. (2018) found that *N*-decanoyl-homoserine lactone (C10-HSL) activated plant systemic resistance against *Botrytis cinerea* in tomato and C10-HSL-induced resistance was largely dependent on the JA signaling pathway [19]. Recently, we demonstrated that 3OC8-HSL primes plant resistance against necrotrophic pathogen *Pectobacterium carotovorum* by coordinating JA and auxin signaling pathway [70]. Therefore, comprehensive studies on the roles of phytohormones such as auxin and JA and their interplay with C10-HSL will shed light on the mechanism by which plants respond to C10-HSL, and will provide insight into novel applications of these biological molecules to regulate crop growth and development.

Materials and methods

Plant growth and chemical treatments

The *Arabidopsis thaliana* ecotype Columbia-0 (Col-0), the mutants *Atmpk6* (obtained from the TAIR stock center), *nia1*, *nia2*, *noa1* (provided by Professor Chunpeng Song in Henan University, China), *rbohD/F* (provided by Professor Zhonglin Shang in Hebei Normal University, China) were used in this study. Seeds were surface sterilized with 75% ethanol for 1 min and 25% bleach for 5 min. After five washes with sterile distilled water, seeds were germinated on agar plates containing half-strength Murashige & Skoog (MS) medium [71] adjusted to pH 5.8. The plates were stratified at 4 °C for 2 days and then placed in a plant growth chamber with a photoperiod of 16 h: 8 h light: dark with 100 $\mu mol \cdot m^2 \cdot s^{-1}$ and temperature of 22±2 °C. Seeds were grown on the vertical position. 3-d-old *Arabidopsis thaliana* seedlings were transferred to half-strength MS medium containing supplemented with various chemicals, including 30 μM C10-HSL, sodium nitroprusside (SNP), 2-(4-carboxyphenyl)-4,4,5,5-tetramethylimidazoline-1-oxyl-3-oxide (cPTIO), hydrogen peroxide (H_2O_2), catalase (CAT), U0126, lithium chloride (LiCl) and lanthanum chloride ($LaCl_3$) and grown for additional 5 d. All chemicals were purchased from Sigma-Aldrich

and C10-HSL was dissolved in ethanol as 30 mM stock solutions.

Analysis of root growth

Seeds were grown on the vertical position. 3-d-old *Arabidopsis thaliana* seedlings were transferred to half-strength MS medium supplemented with the indicated treatments and grown for additional 5 d. Growth of primary roots was measured at the same time every day. After 5 d of treatment, the primary root length was measured using a ruler. Lateral root (LR) number and lateral root primordia (LRP) were determined by counting the lateral roots or LRP present in the primary root, from the tip to the root/stem transition. Lateral root and primordia densities were determined by dividing the lateral root number by the primary root length and expressed as LR cm^{-1} or LRP cm^{-1}. The stage C-D of lateral root primordia according to Zhang et al. (1999) [72] were considered for the research. All experiments were performed with the solvent (ethanol) as a control at an end dilution same as AHL tested.

Immuno-detection of phosphorylated MAPKs

According to the method mentioned by Schikora et al. (2011) [9], total protein was extracted from 3-d-old seedlings pretreated with C10-HSL in half-strength MS medium for additional 5, 15, 30, 45 and 60 min. The total proteins were separated on 12% SDS polyacryl gel. Western blot was done using Phospho-p44/42 MAPK antibody purchased from Cell signaling (CAT. #4370) [9]. Licor-ODYSSEY(CLX) was used to photo blotting images. To obtain higher definition, we used a drawing area function supported by the machine.

Dye loading and laser scanning confocal microscopy

The generation of NO, ROS and Ca^{2+} in root tissue was examined using 4, 5-diaminofluorescein diacetate (DAF-2DA) (Sigma Aldrich), 5-(and-6)-chloromethyl-29, 79-dichlorodihydrofluorescein diacetate (DCF-DA) (Sigma Aldrich) and Fluo-4 AM (Thermo) probes, respectively. Before experiments, roots of seedlings were pre-incubated in the dark in loading buffer (10 mM Tris+50 mM KCL, pH 7.18) containing 5 μM DAF-2DA or 10 μM H2DCF-DA for 30 min, or in buffer (50 mM KCL+10 mM Tris+5 mM $CaCL_2$+0.5 mM eserine, pH 7.18) containing 10 μM Fluo-4 AM for 1 h, and then washed with distilled water to remove excess dye. Examinations of fluorescence intensity were performed using a laser scanning confocal microscope (excitation, 488 nm; emission, 500–550 nm; Leica SP8). For the fluorescence of dyes and GFP, we measured the fluorescence value of all meristematic zone in every plant, using internal Quantity software of Leica SP8 confocal microscope.

RT-qPCR

Total RNA was isolated from root tissues of 12-d-old seedlings treated with the indicated reagents for 0, 1, 3, 6, 12, 24 and 48 h, using Trizol reagent (Invitrogen, Carlsbad, CA, USA). First-strand cDNA was synthesized using Moloney murine leukaemia virus reverse transcriptase (Invitrogen). PCR amplifications were performed according to standard protocols using Taq DNA polymerase or Pyrobest DNA polymerase (TaKaRa). The mean value of three replicates was normalized against that of *ACTIN2*.

$[Ca^{2+}]_{cyt}$ measurements

Arabidopsis seedlings constitutively expressing the aequorin gene were germinated and grown on the half-strength MS agar plates at 23 °C and a 10 h dark/14 h light regime for 10 days. The $[Ca^{2+}]_{cyt}$ rises either as a result of uptake from the extra-cellular space through plasma membrane channels or from the release of internal stores. Roots were incubated in 10 μM coelenterazine (0.1 mM KCL, 1 mM $CaCL_2$,10 mM MES, pH 5.5) for 24 h and rinsed with buffer for 30 min. Each seedling was placed in a luminometer cuvette containing 50 μl buffer solution. C10-HSL stock solution was then injected (50 μl per injection) to achieve the indicated concentration. Final concentrations of $LaCL_3$, verapamil chloride and EGTA were 10 mM, respectively. Thirty pre-washed seedlings were used for each luminometric experiment. Real-time aequorin luminescence was recorded every 1 s over the course of the experiment. At the end of the experiment, 2 M $CaCl_2$ and 10% ethanol were added to discharge any remaining aequorin.

Abbreviations

AHLs	*N*-acyl-homoserine lactones
CAT	catalase C10-HSL:*N*-decanoyl-L-homoserine lactone
cPTIO	2-(4-carboxyphenyl)-4,4,5,5-tetramethylimidazoline-1-oxyl-3-oxide
C6-HSL	*N*-hexanoyl-homoserine lactone
DAF-2DA	4, 5-diaminofluorescein diacetate
DCF-DA	5-(and-6)-chloromethyl-29, 79-dichlorodihydrofluorescein diacetate
GCR	G-protein-coupled receptor
H_2O_2	hydrogen peroxide
$LaCl_3$	lanthanum chloride
LiCl	lithium chloride
LR	Lateral root
LRP	lateral root primordia
MAPK	Mitogen-activated protein kinase
MPK6	*Mitogen-Activated Protein Kinase 6*
NO	nitric oxide
QS	quorum sensing
ROS	reactive oxygen species
SA	salicylic acid
SNP	sodium nitroprusside
3OC8-HSL	3-oxo-octanoyl-homoserine lactone
3OC10-HSL	*N*-3-oxo-decanoyl-homoserine lactone
3OC14-HSL	*N*-3-oxo-tetradecanoyl-homoserine-lactone
3OC16-HSL	3-oxo-*N*-(tetrahydro-2-oxo-3-furaryl)-hexadecenamide

Supplementary Information

The online version contains supplementary material available at https://doi.org/10.1186/s12870-022-03865-6.

Supplementary Material 1: Figure S1. Primary root length and lateral root density of wild-type seedlings exposed to C10-HSL. Figure S2. NIA1, NIA2 and NOA1 participate in C10-HSL induced short primary root. Figure S3. U0126 could rescue C10-HSL induced primary root inhibition. Figure S4. Relative primary root growth of Col-0 seedlings exposed to C10-HSL with or without LiCl plus LaCl3. Table 1. List of the primers for qRT-PCR analysis of the genes. Bloting images (Figure S5 and S6): Original blotting images.

Acknowledgements

We thank Professor Chunpeng Song (Zhengzhou University in China) for providing *nia1*, *nia2*, *noa1* seeds, Professor Zhonglin Shang (Hebei Normal University in China) for providing *rbohD/F* seeds, and the TAIR stock center for the mutants *Atmpk6* seeds. We thank Liwen Bianji (Edanz) (www.liwenbianji.cn) for editing the English text of a draft of this manuscript.

Author's contribution

S.S and C.X. design the experiment and conceived the study. Z.Q. and C.X. is responsible for Figs. 1 and 2; S.Y. is responsible for Fig. 3; C.X. is responsible for Figs. 4, 5 and 7; Z.Z. is responsible for Fig. 6; L.F. and J.Z. manipulate software and participated in data analyzation. S.S.is responsible for all the manuscript. All authors read and approved the final manuscript.

Funding

This work was financially supported by the National Natural Science Foundation of China (Grant Number 31601144) and the Central Guidance on Local Science and Technology Development Fund of Hebei Province(226Z6501G).

Data availability

The datasets used and/or analyzed during the current study are available from the corresponding author on request.

Declarations

Ethics approval and consent to participate

All methods were in compliance with relevant institutional, national, and international guidelines and legislation.

Consent for publication

Not applicable.

Competing interests

We declare that we have no competing interests.

Author details

[1] Biology Institute, Hebei Academey of Sciences, 46th South Street of Friendship, Shijiazhuang 050051, Hebei, China. [2] Hebei Engineering and Technology Center of Microbiological Control on Main Crop Disease, 46th South Street of Friendship, Shijiazhuang, China.[3] College of Life Science, Hebei University, 180th East Road of Wusi, Baoding, China. [4] Hebei Collaboration Innovation Center for Cell Signaling Environmental Adaptation, 20 East NanErhuan Road, Shijiazhuang, China.

Received: 10 May 2022 / Accepted: 20 September 2022
Published online: 14 October 2022

References

1. Steindler L. Detection of quorum-sensing N-acyl homoserine lactone signal molecules by bacterial biosensors. FEMS Microbiol Lett. 2007;266(1):1–9.
2. Williams P. Quorum sensing, communication and cross-kingdom signaling in the bacterial world. Microbiology. 2007;153(12):3923–38.
3. Holm A, Vikstrom E. Quorum sensing communication between bacteria and human cells: signals, targets, and functions. Front Plant Sci. 2014;5:309.
4. Schenk ST, Stein E, Kogel K-H, Schikora A. Arabidopsis growth and defense are modulated by bacterial quorum sensing molecules. Plant Signal Behav. 2012;7(2):178–81.
5. Fuqua C, Greenberg E, Parsek M. Regulation of gene expression by cell-to-cell communication: acyl-homoserine lactone quorum sensing. Annu Rev Genet. 2001;35:435–68.
6. Miller M, Bassler B. Quorum sensing in bacteria. Annu Rev Microbiol. 2001;55:35.
7. Quiñones B, Lindow S, Dulla G. Quorum sensing regulates exopolysaccharide production, motility, and virulence in *Pseudomonas syringae*. Mol Plant Microbe Interact. 2005;18(7):12.
8. Götz C, Fekete A, Gebefuegi I, Forczek ST, Fuksová K, Li X, et al. Uptake, degradation and chiral discrimination of N-acyl-D/L-homoserine lactones by barley (*Hordeum vulgare*) and yam bean (*Pachyrhizus erosus*) plants. ANAL Bioanal Chem Iss. 2007;389(5):1447–57.
9. Schikora A, Schenk ST, Stein E, Molitor A, Zuccaro A, Kogel KH. N-Acyl-Homoserine lactone confers resistance toward biotrophic and hemibiotrophic pathogens via altered activation of AtMPK6. Plant Physiol. 2011;157(3):1407–18.
10. Song S, Jia Z, Xu J, Zhang Z, Bian Z. *N*-butyryl-homoserine lactone, a bacterial quorum-sensing signaling molecule, induces intracellular calcium elevation in Arabidopsis root cells. Biochem Biophy Res Commun. 2011;414(2):355–60.
11. Bai X, Todd CD, Desikan R, Yang Y, Hu X. N-3-oxo-decanoyl-L-homoserine-lactone activates auxin-induced adventitious root formation via hydrogen peroxide- and nitric oxide-dependent cyclic GMP signaling in mung bean. Plant Physiol. 2012;158(2):725–36.
12. Barrera-Ortiz S, López-García C, Ortiz-Castro R, et al. Bacterial quorum-sensing signaling-related drr1 mutant influences abscisic acid responsiveness in *Arabidopsis thaliana*. J Plant Growth Regul. 2022;41(1):376–90.
13. Mathesius U, Mulders S, Gao M, Teplitski M, Caetano-Anolles G, Rolfe BG, Bauer WD. Extensive and specific responses of a eukaryote to bacterial quorum-sensing signals. Proc Natl Acad Sci U S A. 2003;100(3):1444–9.
14. Schuhegger R, Ihring A, Gantner S, Bahnweg G, Knappe C, Vogg G, Hutzler P, Schmid M, Van Breusegem F, Eberl L. Induction of systemic resistance in tomato by N-acyl-L-homoserine lactone-producing rhizosphere bacteria. Plant Cell Environ. 2006;29(5):909–18.
15. Liu F, Bian Z, Jia Z, Zhao Q, Song S. The GCR1 and GPA1 participate in promotion of Arabidopsis primary root elongation induced by N-acyl-homoserine lactones, the bacterial quorum-sensing signals. Mol Plant Microbe Interact. 2012;25(5):677–83.
16. Zhao Q, Li M, Jia Z, Liu F, Ma H, Huang Y, et al. AtMYB44 positively regulates the enhanced elongation of primary roots induced by N-3-oxo-hexanoyl-homoserine lactone in *Arabidopsis thaliana*. Mol Plant Microbe Inter. 2016;29(10):774–85.
17. Morquecho-Contreras A, Méndez-Bravo A, Pelagio-Flores R, Raya-González J, Ortíz-Castro R, López-Bucio J. Characterization of *drr1*, an alkamide-resistant mutant of Arabidopsis, reveals an important role for small lipid amides in lateral root development and plant senescence. Plant Physiol. 2010;152(3):1659–73.
18. Ortíz-Castro R, Martínez-Trujillo M, López-Bucio J. N-acyl-L-homoserine lactones: a class of bacterial quorum-sensing signals alter post-embryonic root development in *Arabidopsis thaliana*. Plant Cell Environ. 2008;31(10):1497–509.
19. Hu Z, Shao S, Zheng C, Sun Z, Shi J, Yu J, et al. Induction of systemic resistance in tomato against *Botrytis cinerea* by *N*-decanoyl-homoserine lactone via jasmonic acid signaling. Planta. 2018;247(5):1217–27.
20. Peng H, Ouyang Y, Bilal M, Wang W, Hu H, Zhang X. Identification, synthesis and regulatory function of the N-acylated homoserine lactone signals produced by *Pseudomonas chlororaphis* HT66. Microb Cell Fact. 2018;17(1):9.
21. Grant J, Loake G. Role of reactive oxygen intermediates and cognate redox signaling in disease resistance. Plant Physiol. 2000;124(1):21–9.
22. Neill S, Desikan R, Clarke A, Hurst R, Hancock J. Hydrogen peroxide and nitric oxide as signalling molecules in plants. J Exp Bot. 2002;53(372):1237–47.
23. Pagnussat G, Lanteri M, Lamattina L. Nitric oxide and cyclic GMP are messengers in the indole acetic acid-induced adventitious rooting process. Plant Physiol. 2003;132(3):1241–8.
24. Niu L, Liao W. Hydrogen peroxide signaling in plant development and abiotic responses: crosstalk with nitric oxide and calcium. Front Plant Sci. 2016;7:230.
25. Zhao Y, Zhang Y, Liu F, Wang R, Huang L, Shen W. Hydrogen peroxide is involved in methane-induced tomato lateral root formation. Plant Cell Rep. 2019;38(3):377–89.

26. Kaya A, Alyemeni M, Ahmad P. Responses of nitric oxide and hydrogen sulfide in regulating oxidative defense system in wheat plants grown under cadmium stress. Physiol Plant. 2020;168(2):16.
27. Zhang P, Luo Q, Wang R, Xu J. Hydrogen sulfide toxicity inhibits primary root growth through the ROS-NO pathway. Sci Rep. 2017;7(1):868.
28. Rankl S, Gunse B, Sieper T, Schmid C, Poschenrieder C, Schroder P. Microbial homoserine lactones (AHLs) are effectors of root morphological changes in barley. Plant Sci. 2016;253:130–40.
29. Liu F, Zhao Q, Jia Z, Song C, Huang Y, Ma H, Song S. N-3-oxo-octanoyl-homoserine lactone-mediated priming of resistance to *Pseudomonas syringae* requires the salicylic acid signaling pathway in *Arabidopsis thaliana*. BMC Plant Biol. 2020;20(1):38–51.
30. Tsuneaki A, Guillaume T. MAP kinase signalling cascade in Arabidopsis innate immunity. Nature. 2002;415:977–83.
31. Zhang A, Jiang M, Zhang J, Tan M, Hu X. Mitogen-activated protein kinase is involved in abscisic acid-induced antioxidant defense and acts downstream of reactive oxygen species production in leaves of maize plants. Plant Physiol. 2006;141(2):475–87.
32. Beckers G, Jaskiewicz M, Liu Y, Underwood W, He S, Zhang S, et al. Mitogen-activated protein kinases 3 and 6 are required for full priming of stress responses in *Arabidopsis thaliana*. Plant Cell. 2009;21(3):944–53.
33. Nguyen X, Hoang M, Kim H, Lee K, Liu X, Kim S, et al. Phosphorylation of the transcriptional regulator MYB44 by mitogen activated protein kinase regulates Arabidopsis seed germination. Biochem Biophy Res Commun. 2012;423(4):703–8.
34. Miransari M, Rangbar B, Khajeh K, Tehranchi MM, Azad RR, Nagafi F, Rahnemaie R. Salt stress and MAPK signaling in plants. In: Ahmad P, Azooz MM, MNV P, editors. Salt stress in plants. *New York*: *Springer*; 2013. pp. 157–73.
35. Ma W, Smigel A, Tsai Y, Braam J, Berkowitz GA. Innate immunity signaling: cytosolic Ca^{2+} elevation is linked to downstream nitric oxide generation through the action of calmodulin or a calmodulin-like protein. Plant Physiol. 2008;148(2):818–28.
36. Han S, Fang L, Ren X, Wang W, Jiang J. MPK6 controls H_2O_2-induced root elongation by mediating Ca^{2+} influx across the plasma membrane of root cells in Arabidopsis seedlings. New Phytol. 2015;205(2):695–706.
37. Jalmi SK, Sinha AK. ROS mediated MAPK signaling in abiotic and biotic stress-striking similarities and differences. Front Plant Sci. 2015;6:769.
38. Zhang W, Zhou R, Gao Y, Zheng S, Xu P, Zhang SQ, et al. Molecular and genetic Evidence for the key role of AtCaM3 in heat-shock signal transduction in Arabidopsis. Plant Physiol. 2009;149(4):1773–84.
39. Cheng Y, Han S, Zhao J, Gao Y, Sun D, Cui S. Calmodulin involved in the cell proliferation of root apical meristem and ABA response in Arabidopsis. Prog Biochem Biophys. 2011;38(1):36–45.
40. Virdi AS, Singh S, Singh P. Abiotic stress responses in plants: roles of calmodulin-regulated proteins. Front Plant Sci. 2015;6:809.
41. Taneja M, Tyagi S, Sharma S, Upadhyay S. Ca^{2+} cation antiporters (CaCA): identification, characterization and expression profiling in bread wheat (*Triticum aestivum* L.). Front Plant Sci. 2016;7:1775.
42. Lombardo M, Graziano M, Polacco JC, Lamattina L. Nitric oxide functions as a positive regulator of root hair development. Plant Signal Behav. 2006;1(1):28–33.
43. Mendez-Bravo A, Raya-Gonzalez J, Herrera-Estrella L, Lopez-Bucio J. Nitric oxide is involved in alkamide-induced lateral root development in Arabidopsis. Plant Cell Physiol. 2010;51(10):1612–26.
44. Moreau M, Lee G, Wang Y, Crane B, Klessig D. AtNOS/AtNOA1 is a functional Arabidopsis thaliana cGTPase and not a nitric-oxide synthase. J Biol Chem. 2008;21(47):32957–67. 283(.
45. Dunand C, Crevecoeur M, Penel C. Distribution of superoxide and hydrogen peroxide in Arabidopsis root and their influence on root development: possible interaction with peroxidases. New Phytol. 2007;174(2):332–41.
46. Tsukagoshi H, Busch W, Benfey PN. Transcriptional regulation of ROS controls transition from proliferation to differentiation in the root. Cell. 2010;143(4):606–16.
47. Beck M, Komis G, Ziemann A, Menzel D, Šamaj J. Mitogen-activated protein kinase 4 is involved in the regulation of mitotic and cytokinetic microtubule transitions in *Arabidopsis thaliana*. New Phytol. 2011;189(4):1069–83.
48. Kosetsu K, Matsunaga S, Nakagami H, Colcombet J, Sasabe M, Soyano T, et al. The MAP kinase MPK4 is required for cytokinesis in *Arabidopsis thaliana*. Plant Cell. 2010;22(11):3778–90.
49. Hubbard KE, Nishimura N, Hitomi K, Getzoff E, Schroeder J. Early abscisic acid signal transduction mechanisms: newly discovered components and newly emerging questions. Gene Dev. 2010;24(16):1695–708.
50. Tewari R, Paek K. Function of nitric oxide and superoxide anion in the adventitious root development and antioxidant defense in Panax ginseng. Plant Cell Rep. 2008;27(3):11.
51. von Rad U, Klein I, Dobrev P, Kottova J, Zazimalova E, Fekete A, Hartmann A, et al. Response of *Arabidopsis thaliana* to N-hexanoyl-dl-homoserine-lactone, a bacterial quorum sensing molecule produced in the rhizosphere. Planta. 2008;229(1):73–85.
52. Ortiz-Castro R, Macías-Rodríguez L, López-Bucio J. The role of microbial signals in plant growth and development. Plant Signal Behav. 2009;4(8):12.
53. Jin G, Liu F, Ma H, Hao S, Zhao Q, Bian Z, Jia Z, Song S. Two G-protein-coupled-receptor candidates, Cand2 and Cand7, are involved in Arabidopsis root growth mediated by the bacterial quorum-sensing signals N-acyl-homoserine lactones. Biochem Bioph Res Commu. 2012;417(3):991–5.
54. Venturi V. Regulation of quorum sensing in Pseudomonas. FEMS Microbiol Rev. 2006;30:274–91.
55. Marketon M, Eberhard A, González J. Characterization of the *Sinorhizobium meliloti* sinR/sinI locus and the production of novel N-acyl homoserine lactones. J Bacteriol. 2002;184(20):5686–95.
56. Palmer A, Senechal A, Mukherjee A, Ane J, Blackwell HE. Plant responses to bacterial N-acyl-L-homoserine lactones are dependent on enzymatic degradation to L-homoserine. ACS Chem Biol. 2014;9(8):1834–45.
57. Campbell R, Greaves MP. Anatomy and community structure of the rhizosphere. In: The Rhizosphere. Chichester. pp.: Wiley; 1990. pp. 11–34.
58. Liu Y, Wang R, Zhang P, Chen Q, Luo Q, Zhu Y, et al. The nitrification inhibitor methyl 3-(4-hydroxyphenyl) propionate modulates root development by interfering with auxin signaling via the NO/ROS pathway. Plant Physiol. 2016;171(3):1686–703.
59. Campos-Cuevas JC, Pelagio-Flores R, Raya-González J, Méndez-Bravo A, Ortiz-Castro R, López-Bucio J. Tissue culture of *Arabidopsis thaliana* explants reveals a stimulatory effect of alkamides on adventitious root formation and nitric oxide accumulation. Plant Sci. 2008;174(2):165–73.
60. Clarke A, Desikan R, Hurst RD, Hancock JT, Neill SJ. NO way back: nitric oxide and programmed cell death in *Arabidopsis thaliana* suspension cultures. Plant J. 2000;24(5):667–77.
61. Kumar KD. Differential induction of tobacco MAP kinases by the defense signals nitric oxide, salicylic acid, ethylene, and jasmonic acid. Mol Plant Microbe Inter. 2000;13(3):347–51.
62. Takahashi F, Yoshida R, Ichimura K, Mizoguchi T, Seo S, Yonezawa M, et al. The mitogen-activated protein kinase cascade MKK3-MPK6 is an important part of the jasmonate signal transduction pathway in Arabidopsis. Plant Cell. 2007;19(3):805–18.
63. Wang P, Du Y, Li Y, Ren D, Song CP. Hydrogen peroxide-mediated activation of MAP kinase 6 modulates nitric oxide biosynthesis and signal transduction in Arabidopsis. Plant Cell. 2010;22(9):2981–98.
64. Takahashi F, Mizoguchi T, Yoshida R, Ichimura K, Shinozaki K. Calmodulin-dependent activation of MAP kinase for ROS homeostasis in Arabidopsis. Mol Cell. 2011;41(6):649–60.
65. Ye Y, Li Z, Xing D. Nitric oxide promotes MPK6-mediated caspase-3-like activation in cadmium-induced *Arabidopsis thaliana* programmed cell death. Plant Cell Environ. 2013;36(1):1–15.
66. Harding SAOS, Roberts DM. Transgenic tobacco expressing a foreign calmodulin gene shows an enhanced production of active oxygen species. EMBO J. 1997;16(6):1137–44.
67. Reddy GB, Reddy PY, Rao GS, Balakrishna N, Srivalli I. Antioxidant defense system and lipid peroxidation in patients with skeletal fluorosis and in fluoride-intoxicated rabbits. Toxicol Sci. 2003;72(2):6.
68. Vanneste SF, Friml J. Auxin: a trigger for change in plant development. Cell. 2009;136:1005–16.
69. Liu W, Li RJ, Han TT, Cai W, Fu ZW, Lu YT. Salt stress reduces root meristem size by nitric oxide-mediated modulation of auxin accumulation and signaling in Arabidopsis. Plant Physiol. 2015;168(1):343–56.
70. Liu F, Zhao Q, Jia Z, Zhang S, Wang J, Song S, Jia Y. N-3-Oxo-octanoyl homoserine lactone primes plant resistance against necrotrophic pathogen *Pectobacterium carotovorum* by coordinating jasmonic acid and auxin-signaling pathways. Front Plant Sci. 2022;13:886268.
71. Murashige T, Skoog F. A revised medium for rapid growth and bioassays with tabaco tissue culture. Plant Physiol. 1962;15:473–97.
72. Zhang H, Jennings A, Barlow PW, Forde BG. Dual pathways for regulation of root branching by nitrate. Proc Natl Acad Sci U S A. 1999;96(11):6529–34.